Plasma Scaling Leads Transition from 2D to true 3D Models

J. Brcka[*1]
[1]Tokyo Electron U.S. Holdings, Inc., U.S. Technology Development Center, 2400 Grove Blvd., Austin, TX 78741, [2]Tokyo Electron
*Corresponding author: Tokyo Electron U.S. Holdings, Inc., 2400 Grove Blvd., Austin, TX 78741, jozef.brcka@us.tel.com

Abstract: A multi-ICP system can be used to increase the plasma uniformity, which makes it possible to increase the processing area and provide additional variables for controlling the plasma. The 3D model of the multi-coil ICP configurations with the asymmetric features is using COMSOL multiphysics software to explore and characterize reactive plasma parameters including their operation in reactive gas. The scaled up reactive plasma 3D simulation is challenging technological, computational, dimensional and chemistry aspects under one framework.

Keywords: 3D plasma simulation, multi ICP, plasma module.

1. Introduction

A multi-ICP (inductively coupled plasma) system can be used for increased area processing and to provide additional variables for controlling the plasma. The ICP sources are meeting demands on efficient low-cost plasma source [1]. In the ICP systems the inductive antenna is coupled to the excited plasma inside the low pressure gas reactor. However, assembling the system from the individual sources is changing the symmetry of the system. Using the multiple antennae the mutual inductance between them and with the plasma can influence the plasma distribution inside the chamber and impact the overall performance of the source. The operation of the multi-source configuration is sensitive either to the return radio frequency (RF) currents in the hardware or inside the plasma.

The simulation of plasmas in technological reactors is typically using an advantage of the axial symmetry in 2D space. However, some systems do not have an ideal axial symmetry. Moreover, the reactor walls are imposing stronger boundary conditions on the distribution of the radicals and by-products in reactive plasmas. The approximation of the asymmetric configuration by the pseudo-symmetric 2D axial models is not good enough to determine plasma distribution and its properties (Fig. 1). In such case it is necessary to explore a full 3D model of the plasma reactor.

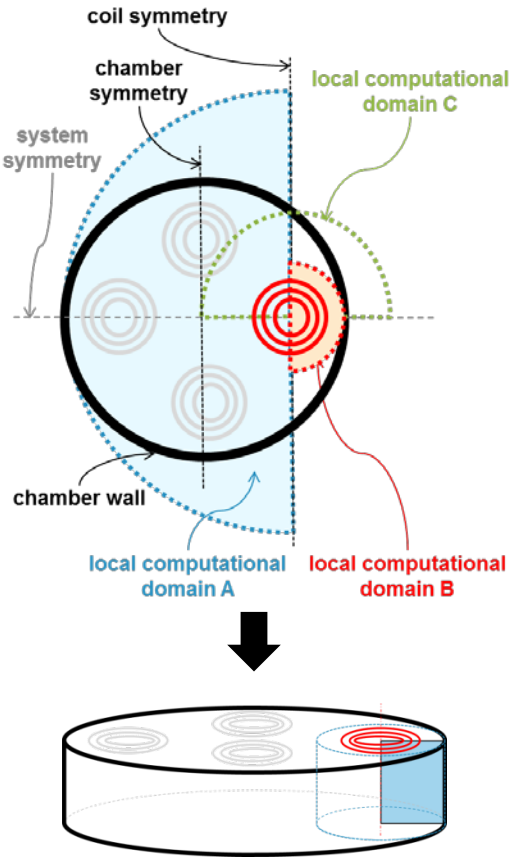

Figure 1. The ICP asymmetric configuration with off-axis antenna used in large reactor is formulated in dual axial symmetry (top) in respect to various boundary conditions at the surrounding walls and full true 3D formulation (bottom).

Scaling the plasma sources is also challenged by the plasma chemistry. To minimize the design and development cost the 3D plasma discharge model with reasonable accuracy is needed to support the prediction of the scaled up plasma tool and processing procedures.

The models of various ICP sources were described elsewhere [2-7]. The numerical simulation techniques commonly used for

simulating low-temperature plasma discharge mainly include the fluid dynamic, kinetic and hybrid models. These models are significantly different in principles, strengths, applications and limitations. The fluid models are used widely for simulation of plasma tools because of its efficient computational cost. This option makes special significance when the technical solution brings additional factors into consideration such are asymmetry, dimensional scale, transient performance, etc. The content and approach in this work is challenging technological, computational, dimensional scaling and plasma chemistry aspects under one framework (Fig. 2).

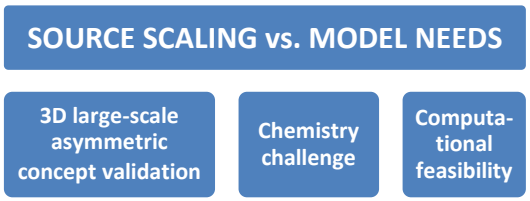

Figure 2. The plasma sources scaling leads a transition in simulation from the models in the 2D-axial symmetry towards the true 3D model concepts.

2. Model description

Plasma simulation is becoming an essential technology used to develop new semiconductor manufacturing equipment and novel process control schemes. While single inductive antenna is coupled only to the plasma, using the multiple antennae the mutual inductance both between other antennae and to the plasma can influence plasma distribution inside the chamber and impact the overall performance of the source.

2.1 Geometry

We formulated a model for multi-ICP in two configurations. The first configuration is represented by **Source A** (Fig. 3) which is consisting of four individual ICP sources arranged around the center of the cylindrical chamber (∅ 860 mm in diameter and 267 mm height) at 90° angle, see also Ref. [8]. Each coil is represented by a spiral (∅5 mm copper tube) with five turns (R_{max}=85 mm, R_{min}=50 mm and 7 mm radial pitch). Figure 4 shows **Source B** that is consisting of the embedded multi-coil structure into a single integrated ICP source at the top of the cylindrical chamber (∅560 mm in diameter and 167 mm height). Each coil is represented by a short single turn spiral (∅5 mm copper tube, R_{min}=50 mm, R_{max}=120 mm, e.g. 70 mm radial pitch). Formally, for modelling purpose the power from the RF generator (13.56 MHz) is delivered to a small section of each coil to establish the identical conditions in the power distribution between the coils. The actual power distribution requires the additional equipment which is not described within the scope of this work. The coils are separated from the plasma by a planar dielectric window.

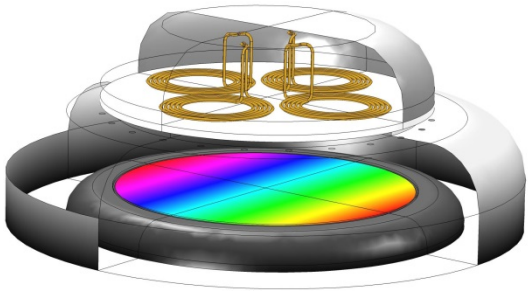

Figure 3. Configurations of the **Source A**: The multi ICP source is composed of four individual ICP sources.

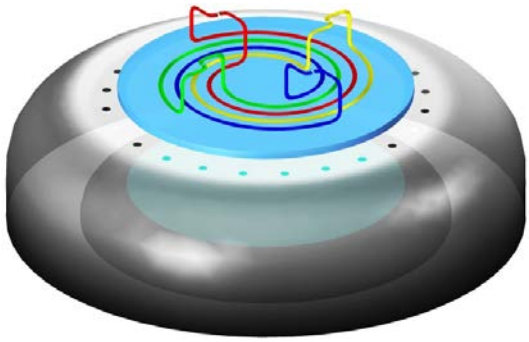

Figure 4. Configurations of **Source B**: The integrated ICP source with embedded multi-coil inductive structure.

2.2 Chemistry

The computational validation of the model was performed with an inert gas – argon. The electron collisions drive the entire processing plasma chemistry and they are among the most important and critical processes that we need to consider. We used limited cross sections for the

reaction scheme (Fig. 5) of the electron-argon collisions that were obtained from Morgan's data at LXCat open-access database [9].

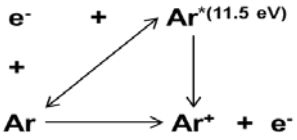

Figure 5. Scheme of the primary electron collisions with argon atoms.

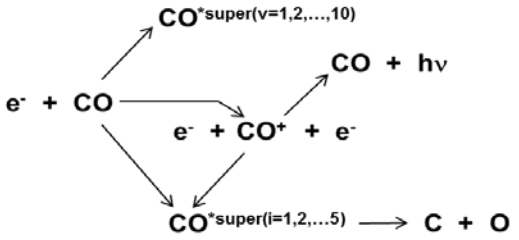

Figure 6. Scheme of the primary electron reactions used in plasma model in the CO gas.

Carbon monoxide, CO, cross section data were downloaded from the website jila.colorado.edu. They contain compilation of Phelps data, and are very similar to the original cross sections by Land [10]. Suggested reaction scheme for CO plasma is shown in Fig. 6. Molecular gases tend to be readily dissociated by electron collisions. We accounted for individual cross sections for published vibrational excitations but a single excited super-molecule $CO^{*super(v)}$ was considered as resultant product, relationship (1) below.

$$CO^{*super(v)} = \sum_v CO^*(v = 1, \dots, 10) \quad (1)$$
$$CO^{*super(i)} = \sum_i CO^*(i = 1, \dots, 5) \quad (2)$$

The major reason to follow this approach was induced by a demand on the computational resources as it will be discussed below in Section 4. Similarly, the electronic excitation state $CO^{*super(i)}$ represents 5 different excitation levels, relationship (2). Considered plasma species in the case of CO molecules, were CO, CO^+, $CO^{*super(v)}$ (all vibrational excitations) and $CO^{*super(i)}$ (all electronic excitations). This approach is somewhat analogic to the principal component analysis used by other researchers [11] to reduce computational demands. The rate coefficients for dissociative recombination (e.g., $AB^+ + e^- \rightarrow A + B$) of the molecular ions CO^+, O_2^+, CH_4^+, CH_3^+, CH_2^+ and CH^+ were obtained from Mitchell [12]. The volumetric electron loss process (collisional radiative recombination) was approximated by net recombination rate [13].

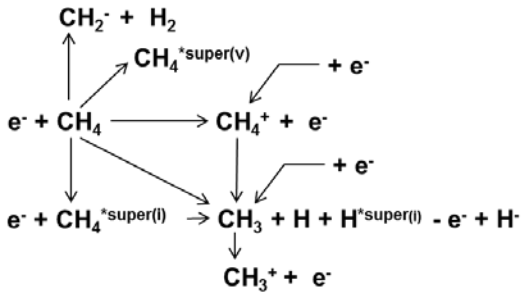

Figure 7. Scheme of the primary electron reactions in the plasma model developed for the methane.

Methane, CH_4, has been the subject of investigation for many years. For instance, Mantzaris et al. [14] developed a self-consistent, 1D simulator for the physics and chemistry of the radio frequency (RF) plasmas. The model for CH_4 chemistry considers four species, CH_4, CH_3 CH_2, and H. The authors determined that CH_4 plasmas are electropositive with negative ion densities one order of magnitude less than those of electrons. The high-energy tail of the electron energy distribution function (EEDF) in the CH_4 is positioned below both the Druyvensteyn and Maxwell distributions. The Maxwell EEDF was used in our model. Also we used a limited reaction scheme (Fig. 7) for CH_4 cross sections [9] and recommendations from work by Morgan [15] and references therein. The following species due to primary collisions with electrons were considered for CH_4 molecules: the ions CH_4^+, CH_3^+, CH_3, CH_4^* vibrational excitations into $\sigma_v(2,4)$ and $\sigma_v(1,3)$ states, and total electronic excitations into $CH_4^{*super(i)}$ leading to dissociation [15]. The super-molecules were considered for excited methane, Eq. (3) and (4).

$$CH_4^{*super(i)} = \sum_i CH_4^*(i) \quad (3)$$
$$CH_4^{*super(v)} = \sum_v CH_4^*(v) \quad (4)$$

The scheme was complemented by CH_4^* (threshold 7.9 eV) excitation cross section and electron attachment, CH_4^-, by Hayashi's data [16]. The species and rates for neutral gas reactions in CH_4 and H_2 (see details in work by Petrov and Giuliani [17]) either unimolecular or bimolecular were not included in the model at this stage and will be considered later together when coupling the plasma model to a heat transfer model.

The excitation of the methane molecules is leading excited $(CH_4)^*$ molecule into dissociation pathways given by Eqs. (5) and (6). Considering proportional branching of these reactions we suggested also to test sub-model that follows the balance due to dissociative recombination given below by relationship (7)

$$e + (CH_4)^* \rightarrow e + CH_3 + H \quad (5)$$

$$e + (CH_4)^* \rightarrow e + CH_2 + 2H \quad (6)$$

$$e + (CH_4)^* \rightarrow e + 0.5CH_3 + 0.5CH_2 + H + 0.5H^* \quad (7)$$

Though, it is not explicitly illustrated in Fig. 7, besides the negative ion of the hydrogen atom, the production of molecular negative ions [9,16] is present, e.g. the CH_4^- and CH_2^-ions. Further, it is assumed either excited or ionized molecules and atoms are recombining at the surface, and radicals are producing parent molecules, thus reproducing neutrals in base state, e.g. formally described by processes

$$(AB)^{exited,ionized} \xrightarrow{surface} AB^0 \quad (8)$$

$$A + B \xrightarrow{surface} AB^0 \quad (9)$$

Considering species and cross sections above does not mean we included all possible collision processes that will occur in the plasma. The proposed scheme is a formal approach to match the actual reaction set but with a limited set of participating species, thus our model is rather limited on chemistry aspects.

3. Use of COMSOL Multiphysics

In this work we implemented commercial Plasma Module of COMSOL Multiphysics (v.4.4 – v.5.0) software [18] for asymmetric ICP reactors both in 2D and 3D versions. We are focusing more on the computational aspects of this approach and technological feasibility we can achieve while dealing with challenges from the introduction section (Fig. 2). The ICP physics interface of Plasma Module helps to set a system of the coupled partial differential equations (PDEs) for the electron density, the mean electron energy, the mass fraction of each of the heavy species, the electrostatic potential, and the electric field due to the induction currents. Plasma Module is automatically supported by the RF module capabilities and Multiphysics solvers. To consider various gas flow path and chemistry the Laminar Flow Module is coupled with Plasma Module in presented models.

4. Simulation results and discussion

To perform our investigation we formulated both the 2D and 3D plasma fluid models under Comsol. The Plasma Module is time-efficient for computation for the most of the 2D ICP models in inert gas with simple chemistry.

Table 1: Range of the computational parameters.

Source A / **Source B**			
Gas chemistry	Ar	CO	CH_4
Required memory resources (GB)	46-49	54	NA
	20-22	25-36	85-90[c] (225)
Typical computation time (hours)	48[a]-193	66	NA
	4[b]-16	10-38	>240[c] (NA)

[a] Within 16 hours – only rare cases with certain level of symmetry

[b] Typically when symmetry level was increased

[c] Not completed due to error related to the limited memory resources

The 3D implementation of the ICP model is computationally more costly. The stationary laminar flow step of the model was solved fast within 6 - 15 min and 13 - 14 GB memory load. However, the transient plasma 3D model was demanding resources according Table 1 and generating unprocessed output files with size around 500 MB and 220 MB in the case of **Source A** and **Source B**, respectively.

For illustration in Fig. 8 a comparison of the 2D pseudo-axial model with true 3D plasma model. Presented geometry is from an equivalent (modified chamber) model of the **Source A**. The 3D model provided more accurate results and reflecting the asymmetry of system. It allowed identifying the plasma parameters within an arbitrary location in a computational domain, e.g. evaluating azimuthal profile. The methane plasma model was under computation at the time of the manuscript submission. The memory demand was around 225 GB for methane chemistry and computational time was estimated well over one week range (data not available due to SW transfer to different machine).

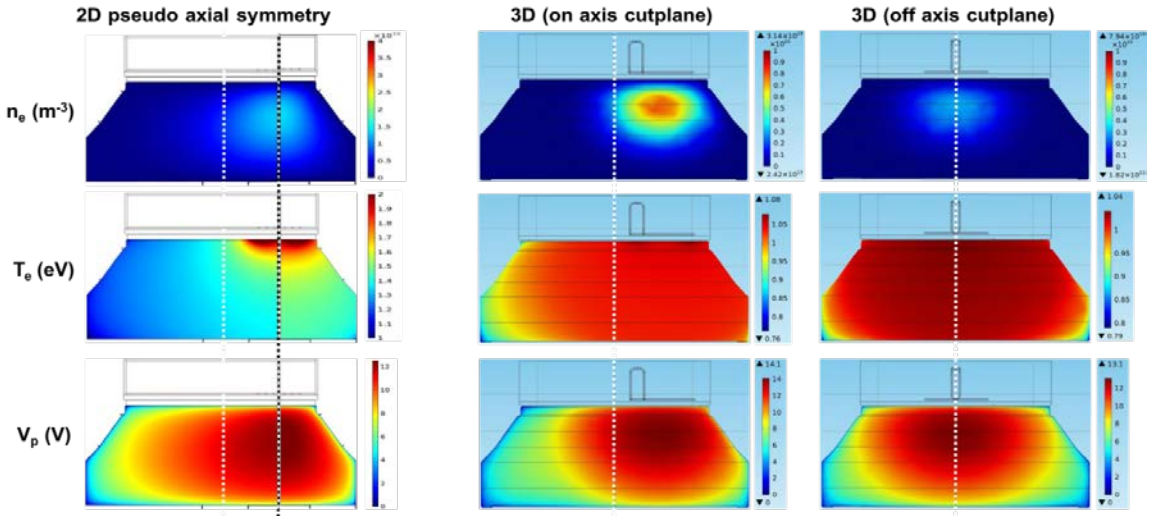

Figure 8. Comparison of the basic plasma parameters in the case of the pseudo-2D axial model (1st column) and the 3D model (2nd and 3rd columns). Single off-axis coil was assumed in these models, see concept from Fig. 1.

4.1 Sweeping operation

The operation of the multi-ICP source [8] can be performed in several modes. The system can run with all coils in parallel connection to the RF generator or to be controlled individually by a controller. The sweeping multi-ICP source is suggested to modify the plasma uniformity in a large-area, low pressure and high-density plasma processing. The described source has capability of azimuthally traveling plasma with various spatial distribution modes in a controlled fashion with potential for large-area high-density plasma applications. Figure 9 illustrates the plasma distribution produced by the **Source A** at various combinations of the ON-OFF status of the RF currents in the coils. Figure 10 illustrates the resistive loses (heating of the plasma) at various operation conditions of the **Source B**. Such conditions are leading towards *in-situ* modification of the plasma distribution. In this case, the plasma distribution is modified accordingly from a non-symmetric distribution towards the uniform and highly symmetric distribution inside the chamber in the dependence on the RF current status on the coils. More work on the features of this source is under current studies and will be published in future [19].

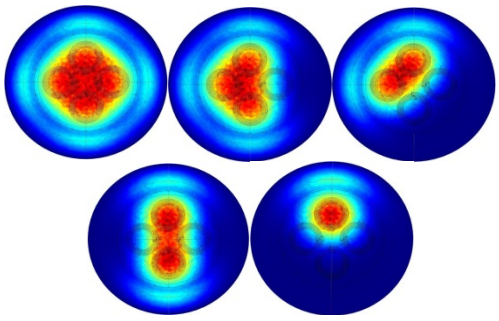

Figure 9. The sweeping plasma concept (ON-OFF currents on the coils to generate moving plasma). The argon plasma density 2D plots in min-max scale at the plane distanced 5 mm from the wafer (50 mTorr, 85 sccm, 5A per coil at 13.56 MHz).

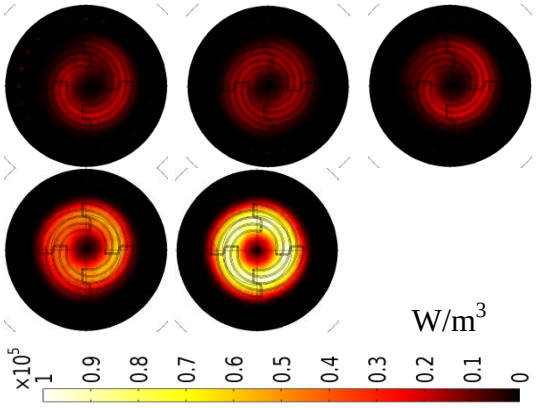

Figure 10. The resistive loses 2D plots (Source B) at the plane 2 mm below the window (50 mTorr, 85 sccm, 5A per coil at 13.56 MHz). The images are in order related to a single coil, the symmetric 2 coils, asymmetric 2 coils, 3 coils and 4 coils.

4.2 Poly-phased operation

In this section a spatial plasma distribution was estimated with respect to the phase applied at each coil. Three baseline configurations were proposed for simulation (Fig. 11) to prove this hypothesis.

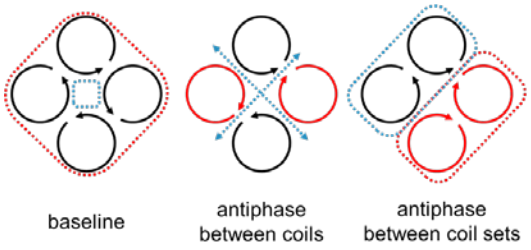

Figure 11. Multi ICP source with poly-phased conditions on the coils.

The baseline case assumed the identical phase on each coil. The antiphase case consisted of π phase difference between the individual coils. The last configuration refers to π phase difference between two sets of coils. There are possible more sophisticated combinations of the phase values on the coils and their sequencies. Figure 12 illustrates the plasma distribution produced by **Source A** at various combinations of the ON-OFF status of the RF currents in the coils. The proposed hypothesis was validated by the simulation profiles.

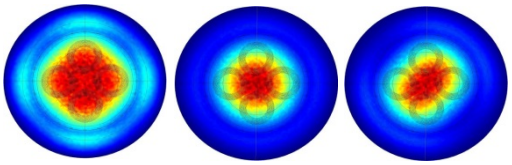

Figure 12. The argon plasma density distribution at plane 5 mm from the wafer for poly-phased conditions. The images are in order related to the baseline (in-phase RF currents), antiphase and grouped antiphase configurations (50 mTorr, 85 sccm, 5A per coil, 13.56 MHz). Min-max scale for color plots is used.

4.3 Chemistry challenge and computational demands

Further investigations were done under increased complexity of the reaction scheme. Initial computations with argon gas, the cases were converging within one to several days (Table 1). However, the chemistry complexity expressed in the number of reactants and possible reactions was a major challenge in solving more complex set of the coupled PDEs. Implementing CO gas detailed chemistry (ten vibrational excitation states, six electron excitation states including dissociative excitation and ionization did saturate operating memory and utilized only several per cent of the computational CPUs power (available 96 GB operational memory and 2x12 CPUs). This reaction setup was not feasible. There are several reasons for that. Firstly, a large number of species led to tremendous memory demand; secondly, a large number of the reactions had an effect on convergence speed. The chemistry challenge was amplified by a large geometrical scale and complexity of the assembly in 3D space. Since, the computational approach is keeping the whole model in memory at once; it requires large memory bandwidth to execute the solvers on the model data in memory. Once memory space is exceeded and solver is accessing overloaded memory storage to pull in more model data, the CPU's performance is decreasing considerably – simply they are not busy at all. Although we explored rather standard settings for solvers without any enhancement tools and optimizations techniques, typically, we had to increase value of the relative tolerance to make case converged. We believe that by optimization of the numerical conditions for

solvers the computational performance might increase substantially.
To reduce the demand on the computer memory we introduced "super-particles" in Section 2.1. This approach allowed higher throughput of the cases. Nevertheless, the computations still had to run at extremely short Δt time steps due to significant volatility of super-particle reaction parameters (we believe these are cross-sections). Compromised solution with clusters of several super-particles worked the most promising within computational framework.

5. Conclusions

Computational framework in 3D geometry allowed prediction of the spatial distributions of plasma and reactants in the asymmetric large-area multi-ICP systems with the support of Plasma Module multiphysics solvers. Selected results were included in this work to document feasibility of this approach. Increased level of the asymmetry is extending computational time, though computational approach provided still reasonable turnover for the most of the computed cases. Large chemistry scale is a remaining challenge and will require a sensitive assessment of the dominant reactions and species to include in models. Full set chemistry in large 3D model would require HPC resources. Nevertheless, we were able to evaluate multiple combinations of the proposed multi-coil ICP configurations in inert gas (including also more difficult chemistry, see carbon monoxide) and generate the transient sequences of the plasma to interpret operation of multi-ICP sources. Global uniformity of the plasma can be controlled by the phase value at the individual coils, thus the multi-ICP configurations can provide a dynamic control of the plasma composition. Furthermore, it is suggested that operation modes have potential to control reaction chemistry and increase radical production.

6. References

1. Tomohiro Okumura, ICP Sources and Applications, *Physics Res. Int. (Hindawi Publishing Corporation,)*, **Volume 2010**, Article ID 164249, 14 pages.
2. M. J. Kushner et al., A 3D model for ICP etching reactors - azimuthal symmetry, coil properties, and comparison to experiments, *J. Appl. Phys.* **80**, 3 (1996).
3. J. L. Giuliani et al., 2D model of a large area, rectangular ICP source for CVD, *IEEE Trans. Plas. Sci.*, **27**, 5 (1999).
4. S. Tinck and A. Bogaerts, Computer simulations of an oxygen ICP used for plasma-assisted ALD, *Plasma Sources Sci. Technol.*, **20** (2011).
5. M. Shigeta, Time-dependent 3D simulation of an argon RF inductively coupled thermal plasma, *Plasma Sources Sci. Technol*., **21** (2012).
6. J. Cheng, L. Ji, K. Wang, Ch. Han, and Y.Shi, Journal of Semiconductors, 34, 6 (2013).
7. K. Ikeda, T. Okumura, and V. Kolobov, "3D simulation for ICP reactor employing multi-spiral coil," *Journal of the Vacuum Society of Japan*, **vol. 50**, no. 6, pp. 424–428, (2007).
8. J. Brcka, Reactive plasmas in multi-ICP system: Spatial characterization by 3D simulation, *The 22nd Int. Symp. on Plasma Chemistry*, July 5-10, 2015, Antwerp, Belgium.
9. Morgan database, www.lxcat.net (retrieved on March 17, 2015).
10. J. Land, J. Appl. Phys. 49, 5716 (1978).
11. A. Berthelot, St. Kolev and A. Bogaerts, 2D self-consistent modelling of an argon microwave plasma over a wide range of pressure. *The 22nd Int. Symp. on Plas. Chem.*, July 5-10, 2015, Antwerp, Belgium.
12. J. B. A. Mitchell, Physics Reports, 186, 215 (1998) cited in: W. L. Morgan, *Advances in Atomic, Mol., and Opt. Physics*, **43**, Academic Press, 102 (2000).
13. M. R. Flannery, in G. W. Drake (Ed.), *Atomic, molecular and optical physics handbook*. AIP, Woodburry, NY (1996).
14. N. V. Mantzaris, E. Gogolides, A. G. Boudouvis, *Plasm. Chem. and Plasm. Processing*, **16**, 3, 301-327 (1996).
15. W. L. Morgan, *Plasma Chemistry and Plasma Processing*, **12**, 4 (1992).
16. Hayashi database, www.lxcat.net , retrieved on March 17, 2015.
17. G. M. Petrov and J. L. Giuliani, J. Appl. Phys., 90, 2 (2001).
18. www.comsol.com, Plasma Module User's Guide.
19. J. Brcka, 3D simulation of integrated multi-coil ICP source with azimuthal modes, *GEC-68*, October 12-16, 2015, Honolulu, USA.